Geotechnical Engineering
(Proceedings of the ICE)

An anchoring system for supporting platforms for wind energy devices

GEEN-2022-245 | Paper

Submitted on: 12-12-22

Submitted by: V Sivakumar

Keywords: ANCHORS & ANCHORAGES, BEARING CAPACITY, PULL-OUT TESTING

An anchoring system for supporting platforms for wind energy devices

V Sivakumar, Queen's University Belfast, UK

J Fanning, Queen's University Belfast, UK

K Gavin, Faculty of Civil Engineering and Geosciences, Delft

S Tripathy, Cardiff University, UK

A Bradshaw, University of Rhode Island, USA

E J Murray, Consultant, Murray Rix Limited, Stoke Golding, UK

J Black, University of Sheffield, UK

S Donohue, University College of Dublin, Southern Ireland

An anchoring system for supporting platforms for wind energy devices

ABSTRACT

This paper presents data from an initial development stage of an 'umbrella anchor' concept. The anchor can be pushed into sand deposit in a folded arrangement to reduce installation loads. When a pull-out load is applied to the anchor's mooring line, the anchor deploys to create a larger embedded plate anchor. Physical modelling was carried out in saturated sand-bed with the anchor installed at depths of up to 1.6m and loaded vertically. During installation, liquefaction was generated at the tip of the anchor to reduce the penetration resistance. This enabled the anchor to be installed quickly and accurately to a target depth. The anchor could provide pull-out resistances comparable to anchor that was wished-in-place at similar depths. The observed behaviour provided encouraging preliminary results and suggests that, with further development and analysis, the concept could potentially be used for commercial applications.

INTRODUCTION

The majority of existing offshore turbines are constructed in water depths between 20-60m (Gavin *et al.,* 2011). As the oil and gas industry moved into areas of deeper water, diverse anchor concepts are being developed (Randolph *et al.,* 2011) to support floating wind turbine platforms. The choice of anchoring system is determined by various factors: size and type of the floating structure, mooring system, seabed conditions and the design life. The anchors commonly known in the industry are anchor piles, suctions caissons, drag anchors, torpedo anchors and plate anchors.

Pile anchors are installed by vibration, driving or drilling and grouting in place. However, the use of these anchors is expensive due to the equipment necessary to install them in deep water. Torpedo anchors behave in the same way as pile anchors. These anchors can be dropped from a known height above the seabed, and they can penetrate the seabed under its self-weight. The final embedment depth and the pull-out capacity of these anchors are difficult to predict but can be determined after installation. However, such installation process may not be feasible in granular deposits or ground with complex geology (Richardson, 2008: Frankenmolen *et al*., 2017). Suction caissons are the most commonly used anchoring systems for various applications both in shallow and deep-water installations due to their ability to resist horizontal and vertical loading and their simple installation and removal processes (Houlsby *et al.,* 2005). Caissons were used as the anchoring system for the world's first grid connected floating turbines for the Hywind project in Scotland.

Plate anchors consist of a fluke which provides the main bearing surface and a central shank which connects the fluke to the mooring line. The plate anchors are installed by dragging them into the seabed. To drag an anchor to a target depth, it may have to be dragged large distances, which will increase site investigation costs and installation time. These anchors provide an efficient option for foundations in terms of their potential pull-out capacity relative to their self-weight. Experimental and numerical investigations showed that the pull-out capacity in both sand and clay varied with anchor shape, soil strength and the depth below the seabed, normalised by anchor width, (Meyerhoff and Adams 1968, Giampa *et al.,* 2019, Jalilivand *et al.*, 2022: Vesic (1971) and Das (1975)). Novel concepts such as the suction embedded plate anchor (Zook *et al.*, 2009), OMNI-Max anchor (Kim *et al.*, 2017), and dynamically embedded plate anchor (O'Loughlin *et al.,* 2014), have been developed in recent years. A concept for an umbrella pile-anchor was developed by the U.S. Naval Civil Engineering Laboratory (1963). The system was designed for conditions in which the installation of piles of sufficient size was impractical or too expensive and the dragging of anchors was limited by space or safety concerns, e.g., due to the presence of buried

infrastructure. The umbrella anchor system proposed in this article is self-installing (with an aid of vibration and liquefaction) thus reducing cost and installation time. It is the intention of the research, presented in this article to see if the proposed mechanism of creating a larger bearing area to enhance pull-out capacity.

ANCHOR CONCEPT

The anchor is designed in the shape of an inverted pyramid (Figure 1). It has four wings that remain in an inverted pyramid shape during installation and then open-up when the anchor is pulled vertically upwards to create a large plate area. The outer edges of the wings are tapered to facilitate the penetration of the wings into the surrounding soil upon pull-out. To enable the four wings to rotate, they were each connected to the central cone through a pin joint as shown in Figures 1 and 2. When the anchor wings are fully deployed, small protrusions on the central cone provide support to the wings as shown in Figure 2. There will be significant bending moments on the wings and shear stresses on the pins and bearing stresses on the support in the proposed design (more discussion later in this article). The guider, shown in Figure 3 was designed to allow the anchor to be pushed into the soil bed. To reduce the forces required for the anchor to be installed, localised liquefaction was generated in the soil. This was achieved by applying a small water jet at a pressure of about 50 kPa to the tip of the anchor. In addition, a vibrating hammer (capacity: 8 J and 50Hz frequency) was attached to the top of the guider to accelerate the installation process. Following the completion of installation and the removal of the follower, a pull-out load was applied to the mooring line.

Analysing plate anchor behaviour in sand

Capacity of a buried plate anchor is dependent on the embedment depth, shape, orientation, loading type and loading angle (in-plane or out-of-plane loading) and the stiffness of the soil (Bradshaw *et al.,* 2016). Murray and Geddes (1987) showed that the anchor pull-out capacity increased as the embedment ratio increased. Centrifuge studies on plate anchors by Ovesen (1981), Dickin and Leung (1992) showed that the pull-out capacities provided by centrifuge modelling were much lower than similar tests carried out under normal gravity (1-g). Ilamparuthi *et al.* (2002) addressed the scaling issues associated with 1-g model tests by using relatively large-scale plate anchors with diameters ranging between 100mm to 400mm.

EXPERIMENTAL PROGRAMME

Nine tests were performed on anchors of two different sizes, inserted at different normalised embedment depths (H/D), where H is the anchor depth and D is the projected or equivalent dimension. In the presentation of the experimental data, two different 'equivalent' dimensions (D) were used, for each of the two different size umbrella anchors investigated. D_1 was

equivalent to the width of the fully opened umbrella anchor (see Figure 4); and D_2 was taken as the diameter of a circular plate of the same total surface area as the four wings of the umbrella anchor. When normalising the anchor depth by D_1, the embedment ratios (H/D) of the tests were between 1.8 and 5.3; and with D_2 based on an equivalent surface area, H/D values were between 2.2 and 6.2. To confirm the capacity and displacement behaviour of the fully opened anchors, tests were also carried out on 'wished-in-place' anchors (placed fully open in the sand bed), for both anchor sizes at the greatest depths of embedment (Table 1). These 'wished in place' tests were also used to verify if the disturbance to the sand bed caused during installation had a noticeable effect on the observed pull-out behaviour.

Anchor geometry and testing chamber

The larger umbrella anchor, UA1, had a width D_1 of 334 mm and surface area of 58,012 mm^2 when fully opened, which equated to an equivalent diameter D_2 based on the surface area of 272 mm (Figures 2 and 4). The smaller umbrella anchor, UA2, had a width D_1 of 223 mm and surface area of 29,006 mm^2 when fully opened, which equated to an equivalent diameter D_2 of 192 mm. The smaller anchor was designed to project a surface area, which was half of the larger anchor, when fully opened. Stainless steel slings with a capacity of 50kN were used as mooring lines to connect the anchor to the load cell.

The follower, shown in Figure 3 used to push the anchor into place, was made using two 800mm long sections of hollow steel tube with an outer diameter of 64mm and wall thickness of 5 mm. The two sections of this follower could be bolted together through a coupling as shown in Figure 3. The follower was split this way in order to make handling of the anchor during installation easy. The lower half of the follower had a lip which allowed the anchor to be placed on the end as shown in Figure 3. This secured the anchor in place during installation and prevented rotation. The water supply line shown in Figure 3 was connected to an outdoor tap with a control on the outlet pressure. The vibrating force was t applied to the top end of the follower, using the vibrating hammer.

The testing chamber used for this work was constructed using four concrete rings (internal diameter 1.2m and highet 0.5m each) and sealed at the joints (Figure 5). A frame was secured using steel square hollow sections and bolted to the top of the concrete rings. A 12V electric car winch with a capacity of 50kN was bolted to the frame. A snatch block was used to increase the load on the anchor by means of strain control at a rate of 2 mm/sec. A 50kN load cell was located in the mooring line and the winch hook as shown in Figure 5 to measure the pull-out force. A cable-extension position transducer was used to measure the displacement of the anchor.

Soil bed preparation

The tests were carried out in beds of fine-to-medium sand which had particle sizes D_{10}, D_{30} and D_{60} of 0.2mm, 0.25mm and 0.35mm respectively. To form a saturated soil-bed the lower section of the chamber was initially filled with water. Sand was then poured into the chamber in layers 300mm thick, with light tamping applied to each layer, to improve the uniformity of the soil-bed. Upon completion of the sand bed, the water level in the chamber was maintained 50 mm above the finished sand surface. For the 'wished-in-place' tests, the anchor was placed fully opened at the required depth and the remainder of the sand bed was formed on top of it.

The peak and ultimate angle of internal friction of the sand were measured in a shear box under a vertical pressure of 15 kPa (average vertical effective stress in the sand when the chamber was full) and the relevant values are 40° and 37° respectively. The dilation angle was 4 degrees at the peak stress.

A cone penetrometer was manufactured, for this research at Queen's University Belfast, to establish the uniformity of the sand beds (Figure 6). The cone had a tip angle of 60° and surface area of 1,500 mm^2. This cone was pushed into the soil-bed at a slow rate (2mm/sec), and the force on the cone was measured using a load cell located above the cone as illustrated in Figure 6. Before the installation of the anchor, cone penetrometer tests were carried out in the centre of the sand bed. The cone penetrometer tests were carried out in the middle of the sample, because this area would be disturbed by the installation of the anchor. For the 'wished-in-place' anchor tests, the cone penetrometer tests were carried out before the pull-out tests at a point 300mm from the chamber wall. In this case, to reduce any rotation of the anchor due to disturbances of the sand caused by installing and removing the cone penetrometer, the cone was inserted only to half the depth of the buried anchor. It was assumed that if the tip resistance to this depth agreed with the other tests, it was reasonable to consider the properties of the soil-bed were comparable to the other tests.

The profiles of cone tip resistance with depth for each test are shown in Figure 7. Due to limitations of the test equipment, profiles could only be taken to a maximum depth of 1600mm. The tip resistance linearly increased with depth. The consistency of the tip resistance among nine test beds was good and confirmed the uniformity of the soil beds prepared for the investigations. Using the measured tip resistance and the empirical model, proposed by Kim *et al.* (2016), the relative density of the sample was estimated to range from 47% at a depth of 200mm to 56% at 1600mm.

After the anchor was installed to a required depth, pull-out tests were performed. The vertical displacement, H* (Figure 4), required for the anchor wings to fully open is approximately 134 mm in the case of UA1 and 74 mm in the case of UA2. These displacements are based on the geometry presented in Figure 4. However actual vertical displacement required for the wings to open could be higher than these values due to small deformation of the soil above the wings during initial pull-out. The wished-in-place anchors were located slightly lower embedment depths than the dynamically installed anchors (by 134 mm for UA1 and 74 mm for UA2) so that the H/D ratio after full-opening would be approximately same for both installation methods.

The guider was removed upon reaching the required depth and the mooring line was then attached to the winch and subjected to a small amount of tension. Figure 8 shows images of the unearthed anchors. Figure 8(a) shows the top end of the closed anchor, after installation, but without a pull-out load applied to the anchor. Figure 8(b) was taken after a test had been completed and the anchor unearthed. This confirmed that the anchor wings had fully opened with the application of a pull-out load.

PREDICTIVE MODELS

The space between the fully opened wings (W in Figure 4) ranges from 15 mm to 127 mm for UA1 and 15 mm to 80 mm for UA2. The angle between the wings was approximately 41 degrees. Due to the small size of these gaps, the failure zones of each anchor wing would interact with each other upon pull-out. The combined zone above the anchor wings would fail as one overlapping or composite mechanism as opposed to four separate failure zones. This behaviour of interfering anchor plates has been examined in the past by Geddes *et al.* (1995) and Kumar *et al.* (2008) and highlights a simplification in assuming equivalent circular plate anchors for the analysis of the umbrella anchor loading capacities. This assumption is appraised and expanded upon further in the following sections.

Plots of pull-out capacity for plate anchors are frequently presented in terms of breakout factors, N_q and this approach is adopted herein. The measured pull-out forces were converted to breakout factors using the following equation.

[1] $$N_q = \frac{q_u}{\gamma' H}$$

where q_u is the pull-out forced divided by the anchor area, γ' is the effective unit weight of the sand and H is the depth of the anchor below the soil surface. To appraise the effect of the gaps between the opened wings, while not knowing the exact failure mechanism, the measured pull-out capacities of each anchor were plotted as two different breakout factors using the corrected diameters, D_1 and D_2, described earlier. Analytical methods for shallow circular plate anchors presented by Murray and Geddes (1987) and Ilamparuthi *et al.* (2002) were used to predict the anchor capacity achieved by the umbrella anchors. It is recognised that other methods are available in the literature, however, for this feasibility assessment the methods were adopted due to the relatively simplicity.

Murray and Geddes (1987) proposed an Upper Bound plasticity solution adopting an associated flow rule material (where the angle of dilation equals the angle of friction) to predict N_q.

[2] $$N_q = 1 + 2\frac{H}{D}\tan\Phi' \left(\frac{2}{3}\frac{H}{D}\tan\Phi' + 1\right)$$

Whilst Ilamparuthi *et al.* (2002) proposed a series of empirical equations (Eqs. 3-9):

[3] $N_{qf} = e^{(33.5/28)(H/D)}$ for 0.0 ≤ H/D ≤ 1.0

[4] $N_{qf} = (H/D)N_{qf1}$ for 1.0 < H/D ≤ 2.4

[5] $N_{qf} = (H/2D)\left(e^{tan\Phi.\ln(H/D)}\right)N_{qf1}$ for 2.4 < H/D ≤ 4.2

[6] $N_{qf} = \left[(H/D) + (H/D)\left(e^{tan\Phi.\ln(D/H)}\right)\right]N_{qf1}$ for 4.2 < H/D ≤ 6.0

[7] $N_{qf} = \left[(H/D) + \left(e^{tan\Phi.\ln(H/D)}\right)\right]N_{qf1}$ for 6.0 < H/D ≤ 10.0

[8] $N_{qf} = \left[N_{qf10} + e^{tan\Phi.\ln(H/D - 10)}\right]$ for 10.0 < H/D ≤ 12.0

[9] $N_{qf}^{\Phi} = N_{qf}^{33.5}\left[e^{(H/3D)(\Phi - 33.5)/33.5}\right]$

where Φ' is the friction angle.

In these equations, N_{qf} is the breakout factor for an anchor in loose sand with Φ' = 33.5° and N_{qf1} and N_{qf10} are the breakout factors for H/D = 1.0 and 10 respectively. Equation [9] can be used to predict a breakout factor N_{qf}^{Φ} for any embedment ratio and friction angle for denser sands. Ilamparuthi *et al.* (2002) postulated that transitional behaviour (i.e. from shallow failure to deep failure) occurred at embedment ratios varying from 4.8-6.8 depending on the density of the sand.

RESULTS

Anchor capacity

Figure 9 shows a comparison of the break-out factor, N_q, against the anchor displacement, δ normalised by D_2 for 'wished-in-place' and dynamically installed anchors with H/D of about 6. It could be asked if the wings of the dynamically installed anchors open-up at the pre-determined vertical displacement based on the geometry of the anchors. To assess this, simple graphical constructions (broken grey lines in Figure 9) were carried out to estimate the vertical displacements at which the wings fully opened (Figure 9). Approximate values of vertical displacement are 132 mm and 82 mm for UA1 and UA2 respectively. These displacements are in close agreement with the theoretical values based on the geometry of the anchors (H*, Figure 4).

For the 'wished-in-place' tests, the pull-out forces on the anchors steadily increased to a maximum pull-out capacity, N_q of 30 and 41 for UA1 and UA2 respectively. However, the dynamically installed anchors showed slightly different responses. N_q increased slowly to a value of approximately 10 at a normalised displacement of 0.48 which corresponds to displacements of 127 mm and 92 mm for UA1 and UA2 respectively. These displacements are approximately equal to the vertical height H* of the anchor wings when fully closed (Figure 4). The breakout factors for UA1 and UA2 were 32 and 42 at normalised displacements of approximately 0.7 and 1.2 respectively. The capacity of the dynamically installed and 'wished-in-place' anchors are in close agreement, which gives confidence to the proposed analytical method of anchoring system for supporting offshore structures. This would also suggest that minimal disturbance occurred to the soil bed as a result of installation and opening of the anchor.

Figures 10 and 11 show the effect of H/D on the normalised load-displacement plots for all tests performed for UA1 and UA2 respectively. All tests show the occurrence of a step in the load, as the anchor wings deployed, followed by an increase in load and a peak resistance similar to the wished-in-place tests. To fully open, both anchor sizes required a vertical displacement of about $0.5D_2$ (diameter of the equivalent circle) or $0.4D_1$ (width of the fully opened anchor) as shown in Figures 10 and 11. The load-displacement plots give no indication that the embedment depth had an effect on this opening distance. All tests showed a peak in anchor capacity, which then decreased, due to the reduction in confining and overburden pressures as the anchor mover upwards.

The peak pull-out capacity factors achieved at different embedment ratios for UA1 – the larger anchor size - are shown in Figure 12, along with the predicted capacities calculated from existing studies, using the peak angle of internal friction. The observed breakout factors show that pull-out capacity increases with embedment ratio as expected. When the actual area of the anchor is used to determine the bearing capacity factor, and the equivalent diameter D_2 is used to determine the embedment ratio, the observed capacity is close to that predicted by Murray and Geddes (1987) and Ilamparuthi *et al.* (2002) up to an embedment ratio of around 4.8. The maximum difference between predicted and measured values is around 7%. The tests carried out at embedment ratios greater than this provided capacities which were lower than expected. As discussed earlier, embedment ratios of 4.8 and 6.8 are typical values for the transition behaviour from shallow to deep failure mechanism in loose and dense sand (Ilamparuthi *et al.,* 2002 and Meyerhof and Adam, 1968). It should also be noted that the transition limits are dependent on anchor shape and size, and boundary effects. The case presented in this investigation is not typical as there were four, irregularly shaped wings. However, they all were connected via the same pull-out unit. The sand bed used in the investigation was loose to moderate dense. Assuming that the model predictions reported by Murray and Geddes (1987) and Ilamparuthi *et al.* (2002) are reasonable estimates for the pull-out capacities, it could be expected that the transition behaviour to be at L/D ratio of 4.8, assuming the sand bed was loose. Based on the equivalent diameter D2, it appears, as shown in Figure 12, that the transient behaviour takes place around H/D ratio of 4.8. However, for H/D ratio based on the actual width of the anchor, the transition behaviour took place at H/D ratio of about 3.9 (Figure 12), which may not be realistic. In essence, it is difficult to assign an "equivalent diameter" to an anchor unit having a complex shape. Nevertheless, it appears that, a deep failure mechanism may have occurred in UA1 at lower H/D ratio lower than could be expected in loose to medium sand. A reason for such a behaviour can be attributed to possible boundary effects caused by the concrete cylinder that contained the sand which diameter was only 3.6 more than the width of the anchor unit.

Figure 13 shows the normalised capacity for UA2 – the smaller anchor - at varying embedment ratios along with the predicted capacities. When the anchor capacity and embedment ratio were normalised using the actual anchor area and equivalent diameter, the observed capacity was close to that predicted by Murray and Geddes (1987) and Ilamparuthi *et al.* (2002). It should be noted that the predicted results exceed the measurements beyond an embedment ratio of 5. When the anchor's projected area and full width D_1 are used to normalise the results in the UA2 tests, the capacity achieved is generally less than the predicted values. The notable reduced increase in anchor capacity observed at the greatest embedment ratios for the UA1 tests did not occur for UA2 which was earlier attributed to a possible boundary effect, triggering

a premature deep failure mechanism. In UA2, boundary effects are significantly less since the size of the anchor (based on width) 5.4-fold less than the diameter of the concrete cylinder housing the sand.

DISCUSSION

Potential Field Application

The initial application of the anchor was assessed in granular soils such as fine-to-medium SAND. Since the installation procedure heavily relies upon “liquefaction effects”, the proposed anchor mechanism is only suitable to be used in silt and up to medium sand. It will not be effective in coarse sand and gravel. However, it can also be used in clay deposits with a soft to firm consistency. The anchor installation procedure, using a simple vibrating mechanism and water jetting facility proved successful, as installation of the anchor to a depth of 1.6m could be readily achieved in minutes, by a single operator. It was found that as the anchor penetrated further into the sand bed the required installation effort reduced significantly. It could be due to excess pore pressure being generated by the vibrations (liquefaction effects) and insufficient time for it to dissipate due to a long drainage path, although the sand bed was highly permeable. In the case of sand deposit, cavity formation behind the anchor during installation, was not found to be an issue.

There are two other concerns in the current form of the anchor design: (a) a significant bending moments and shear stresses can occur at the points where the anchor plates are supported and (b) possibility of buckling of the follower. The structural stability of the umbrella anchor in practical applications is of paramount importance. Notably, bending stresses in the wings under operational conditions can be assessed from the bearing capacity calculations and the likely eccentricity of the loadings. Other potential structural issues are; pin failure under shear and bearing failure under the supporting protrusion (Figure 1). A complete structural analysis is therefore necessary prior to a potential investigation of a protype anchor system. However, preliminary calculations have shown that (for the configurations used in this investigation) the shear loading on each of the supporting protrusion and pin in UA1 at a deepest embedment ratio can be as high as 5.0 kN and about 0.56kNm of bending moment on the plate. The most obvious failure of the system could be associated with the pins. The pins (diameter 8 mm) were made of mild steel and based on the yield stresses, under the current loading conditions the factor of safety against shear failure is approximately 7. The shear loading and the bending moment can be reduced significantly by having chain links between the wings and the extended central shaft as shown in Figure 14. Such an addition to the proposed anchor system

will not interfere with the installation process as the chains will be contained within the folded wings.

Pull-out Capacity

The behavioural trends of the bearing capacity factors for both anchor sizes were generally reasonably consistent with the trends predicted by Murray and Geddes (1987) and Ilamparuthi *et al*. (2002). There were however disparities between the predicted and actual behaviour at the greatest depth of embedment for test series UA1 for the larger anchor. The authors believe that the anchor at this depth behaved as a deep anchor, thus the current models do not reflect the actual behaviour of the subsoil. The predictions also tend to exceed the experimental evidence of the UA2 smaller anchor test series when $D = D_1$. This is not wholly surprising as the analytical approach of Murray and Geddes (1987) should provide an Upper Bound solution.

It is suggested that the overlapping failure mechanism of the individual anchor wings caused the sand above the anchor to fail as one complex mechanism, and there appears to be some justification for developing an analysis based on equivalent circular plate anchors though further research is needed to fully investigate the concept. There are a number of other factors that need investigating, in developing the system. These include: the effects of anchor inclination and loading angle; the effects of repeated cyclic loading on pull-out capacity; suction effects behind the anchor, particularly under rapid dynamic loading. Other factors of interest are possible liquefaction in front of the anchor due to vibrations and oscillations in loading; exploration of the behaviour is fine subsoils and extending the predictive analyses for shallow and deep anchors to full-scale prototype anchors.

Scale Effects

Although no specific prototype size was specified, it is anticipated that ratio of model to prototype scale could be on the order of 1:5. The present physical modelling involved two steps including (i) installation of the anchor by a combination of jetting at the anchor tip to liquefy the soil along with vibratory driving, and (ii) application of pull-out loads to the anchor after installation. Scale effects associated with anchor pull-out can be more easily addressed. However, the major limitation of reduced scale 1g testing is that the stresses in soil do not scale with geometry, which can affect the soil constitutive response. It is expected that monotonic loading of the model anchor occurred under drained conditions. If the model soil is prepared to the same relative density as the prototype, the model soil will have higher dilation and strength due to the lower confining pressures. The loads and displacements will also be lower in the model. Previous 1g studies on plate anchors (e.g., Bradshaw *et al.,* 2016) and

other foundations (e.g., Kelly *et al.,* 2006, LeBlanc *et al.,* 2010) have addressed these effects by: (i) presenting the load test results in terms of non-dimensional quantities, and (ii) preparing the soil looser in the model than in the prototype such that the soil has the same dilation response and peak friction angle. The soil friction angle in the physical model in this study was estimated to be 40 degrees based on element tests performed at comparable void ratios and confining pressures. Cone testing suggested that the soil had a relative density of around 50%. Therefore, the dimensionless model test results should be representative of a prototype anchor embedded in sand with a friction angle of 40 degrees. Since the confining pressures in the prototype will be higher, and thus more contractive, the relative density in the prototype would be higher, on the order of 65% for a scale factor of 5 for example, to achieve the same dilatancy index (Bradshaw *et al.,* 2016).

CONCLUSION

This paper reported data from an initial development stage of an 'umbrella anchor' concept, where the anchor was pushed into sand deposit in a folded arrangement to reduce installation loads and it opened-up upon applying pull-out load to generate a large bearing area. The investigations were carried out in a large concrete chamber housing fine sand placed in loose to moderate dense state. The installations methods (in the form of vibration and liquefaction induced by jetting) adopted in the investigations found to be straightforward and can be adopted in full-scale application.

Upon the application of a vertical pull-out load, the anchor deployed as expected to create a large, embedded plate area. This was verified by unearthing the anchor after peak pull-out capacity had been achieved. The load-displacement behaviour of the anchors during withdrawal also indicated opening of the anchor occurred in all tests. This was evidenced by the temporary plateau in the load capacity prior to the anchor being fully open and reaching peak pull-out capacity. The vertical displacement required to fully open the anchors did not appear to be dependent on the embedment depth but was a function of the anchor geometry. At greater depths, the plateau in the pull-out load caused by the opening of the anchor was less pronounced due to increased overburden stress within the soil-bed.

Further research is necessary in order to validate the application of the concepts at larger scales. Refinement of the anchor design is also necessary, in order to reduce the apertures between the anchor wings when fully opened. The load carrying capacity of the anchors can be reasonably appraised using existing method of analysis for equivalent circular anchor plates, though further research is required to refine the accuracy of the methods, including scale and the boundary effects.

ACKNOWLEDGEMENT

The funding for the project was provided by the Department for Learning and Employment, NI, UK under the US-Ireland R&D partnership. Grant No USI-041.

REFERENCES

Bradshaw, A.S., Giampa, J.R., Gerkus, H., Jalilvand, S., Fanning, J., Nanda, S., Gilbert, R., Gavin, K., and Sivakumar, V. (2016). "Scaling Considerations for 1-g Model Horizontal Plate Anchor Tests in Sand." *Geotechnical Testing Journal,* ASTM, 39(6), 1006-1014.

Das, B. M. & Seeley, G.R. (1975). Breakout resistance of shallow horizontal anchors. Jnl. Geotech. Eng. Div, Proc. ASCE, 101, GT9, 999-1003.

Dickin, E. A. (1988). Uplift behaviour of horizontal anchor plates in sand. J. Geotech. Engineering 114, No. 11, 1300–1317.

Frankenmolen, S., Erbrich, C.T. and Fearon, R. 2017. Successful installation of large suction caissons and driven piles in carbonate soils. In proceedings of 8th international conference on offshore site investigation and geotechnics. Society for Underwater Technology, London, pp 539-548.

Gavin, K., Igoe, D., & Doherty, P. (2011). Piles for offshore wind turbines: A state-of-the-art review. Proceedings of the Institution of Civil Engineers: Geotechnical Engineering, 164(4), 245-256

Giampa, J., Bradshaw, A Gerhus, H, Gilbert, R. Gavin, K, and Sivakumar, V. 2019, 23. The Effect of Shape on the Pull-out Capacity of Shallow Plate Anchors in Sand, Geotechnique Vol. 69, No. 4, pp 355-363.

Houlsby, G.T and Byrne, B.W., 2005. UK Design procedures for installation of suction caissons in clay and other materials, Proceedings of the Institution of Civil Engineers Geotechnical Engineering, No. 2, pp75–82

Jalilvand, S., Gavin, K.G. Sivakumar, V, Gilbert, R. and Bradshaw, B. 2022, 3. New insights into the failure mechanisms of horizontal plate anchors in clay during pull-out, Geotechnique, Vol. 72, Issue 3, pp 189-199.

Ilamparuthi, K., Dickin, E. A. & Muthukrisnaiah, K. (2002). Experimental investigation of the uplift behaviour of circular plate anchors embedded in sand. *Canadian Geotechnical Journal*, 2002, 39:648-664.

Kelly, R.B., Houlsby, G.T., and Byrne, B.W. (2006). "A comparison of field and laboratory tests of caisson foundations in sand and clay." Geotechnique, 56(9), 617-626.

Kim, Y. H. & Hossain, M. S. (2017). Dynamic installation, keying and diving of OMNI-Max anchors in clay. Géotechnique 67, No. 1, 78–85, [http://dx.doi.org/10.1680/jgeot.16.T.008].

LeBlanc, C, Houlsby, G.T., and Byrne, B.W. (2010) "Response of stiff piles in sand to long-term cyclic lateral loading." Geotechnique, 60(2), 79-90.

461 Meyerhof, G. G. & Adams, J. L. (1968). The ultimate uplift capacity of foundations. Canadian
462 Geotechnical Journal 5, No. 4 2225-244.
463 Murray, E. J., & Geddes, J. D. (1987). Uplift of anchor plates in sand. Journal of Geotechnical
464 Engineering, 113(3), 202-215.
465 O'Loughlin C.D., Blake A.P., Richardson M.D., Randolph M.F. and Gaudin C. (2014).
466 Installation and capacity of dynamically embedded plate anchors as assessed through
467 centrifuge tests. Ocean Engineering 88 (2014) 204–213.
468 Ovesen, N. K. (1981). Centrifuge tests on the uplift capacity of anchors. Proc. 10th Int. Conf.
469 Soil Mech. Found. Eng, Stockholm 1, 717–722.
470 Randolph, M., Gourvenec, S. White, D, and Cassidy, M (2011), Offshore geotechnical
471 engineering, Spon Press.
472 Richardson, B.E., 2008. Dynamically installed anchors for floating offshore structures, Thesis
473 presented for the degree of DOCTOR OF PHILOSOPHY, The University of Western
474 Australia
475 Sutherland, H.B. (1965). Model studies of shaft raising through cohesionless soils. *In*
476 Proceedings of the 6th International Conference on Soil Mechanics and Foundation
477 Engineering, Montréal, Vol. 2, pp. 410–413.
478 Tagaya, K., Scott, R.F., and Aboshi, H. 1988*a*. Scale effect in anchor pull-out test by
479 centrifugal technique. Soils and Foundations, **28**(3): 1–12.
480 U.S. Naval Civil Engineering Laboratory (1963) *Umbrella-Pile-Anchors*, Defence Technical
481 Information Centre.
482 Vesic, A. S. (1971). Breakout resistance of objects embedded in ocean bottom. Journal of the
483 Soil Mechanics and Foundations Division 97, No. 9, 1183-1205.
484 Zook, J.R. and Keith, A.L. (2009) Improvements in Efficiency for Subsea Operations in
485 Deepwater Angola. In: Proceedings of the SPE/IADC Drilling Conference and Exhibition,
486 SPE-119651-MS. Amsterdam, The Netherlands
487
488
489

Table 1 Summary of testing schedule

Test Number	Embedment ratio (H/D) where D=B	Embedment ratio (H/D) where D is based on the equivalent area	Test type	Anchor size
1	4.8	5.9	Wished-in-place	UA1
2	4.9	6.1	Installed & loaded	
3	3.9	4.8	Installed & loaded	
4	2.5	3.1	Installed & loaded	
5	1.8	2.2	Installed & loaded	
6	5.2	6.0	Wished-in-place	UA2
7	5.3	6.2	Installed & loaded	
8	4.2	4.9	Installed & loaded	
9	2.7	3.1	Installed & loaded	

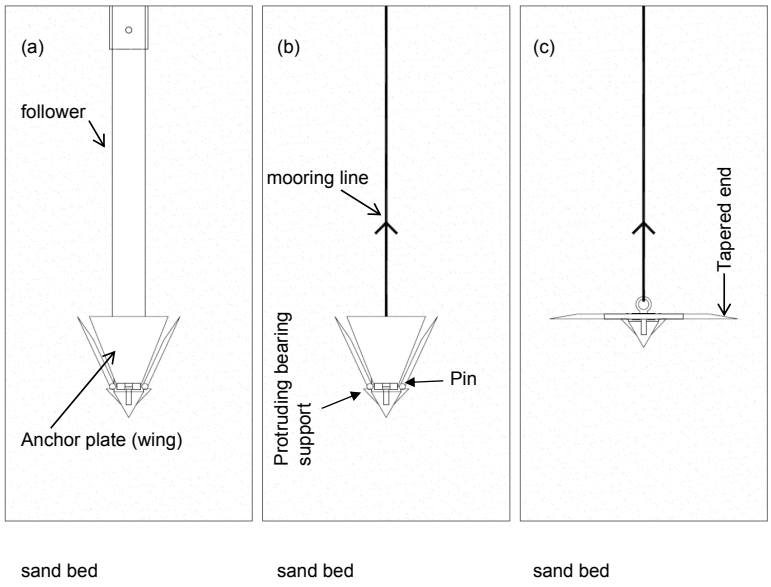

Figure 1. Umbrella anchor installation (a) anchor is pushed into place using the follower with the mooring line through the centre of the follower, (b) follower is removed and pul-lout force applied to the mooring line (c) anchor moves vertically and opens to create an embedded plate anchor

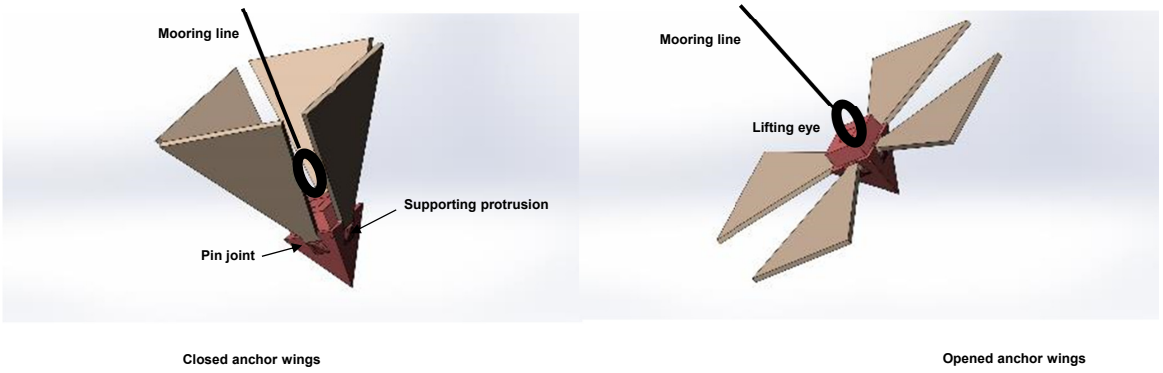

Figure 2. Umbrella anchor

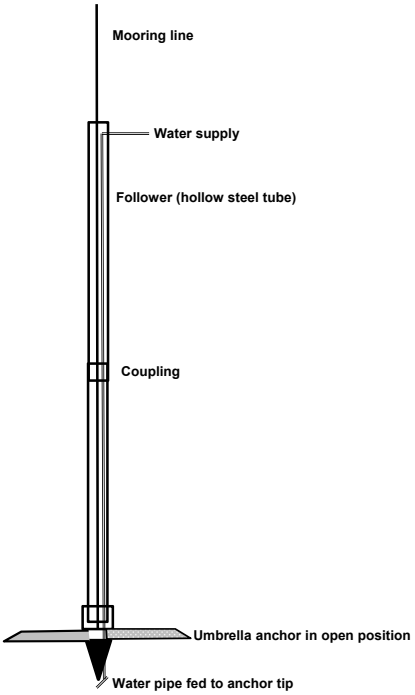

Figure 3. Follower with anchor attached

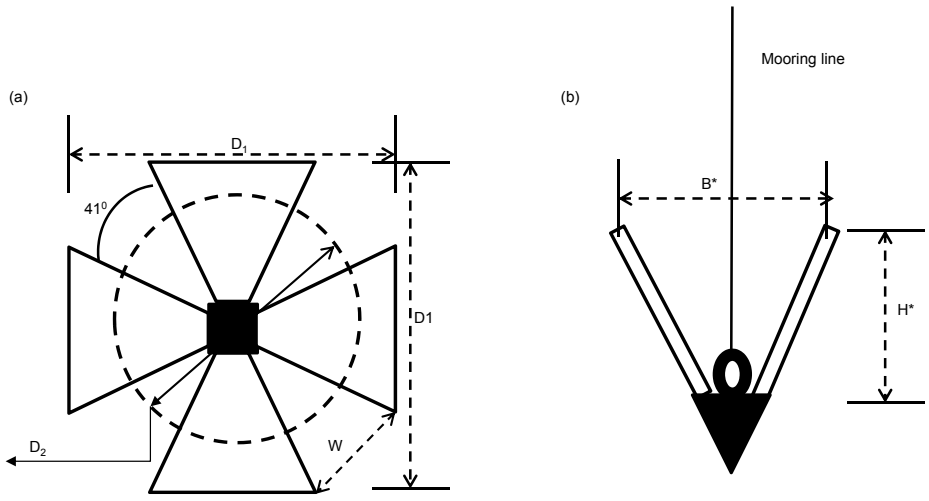

UA1
D_1 = 334 mm; D_2 = 272 mm ; W = 127 mm; B* = 199mm; H*= 134 mm

UA2
D_1 = 223 mm; D_2 = 192 mm; W = 80 mm; B* = 144mm; H*= 74 mm

Figure 4. Umbrella anchors used in testing with dimensions. (a) Plan view of opened anchor and (b) Section of closed anchor

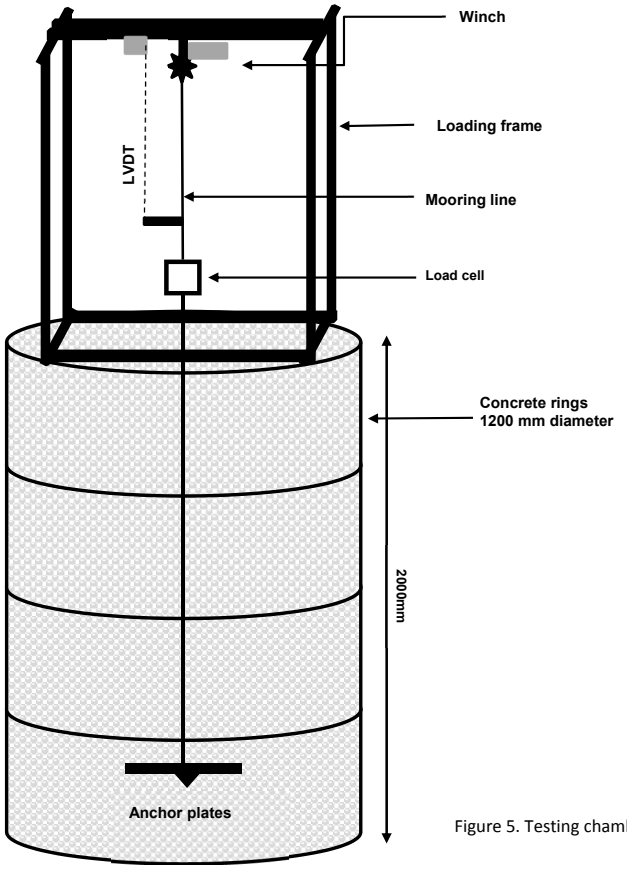

Figure 5. Testing chamber, loading frame and instrumentation

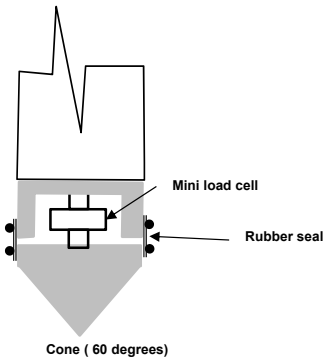

Figure 6. Diagram of cone penetrometer used in testing

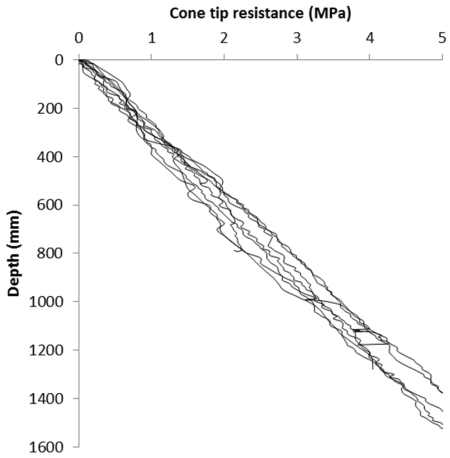

Figure 7. CPT profiles

(a) (b)

Figure 8 Photos of the unearthed anchor (a) closed after installation and (b) fully opened after pull-out

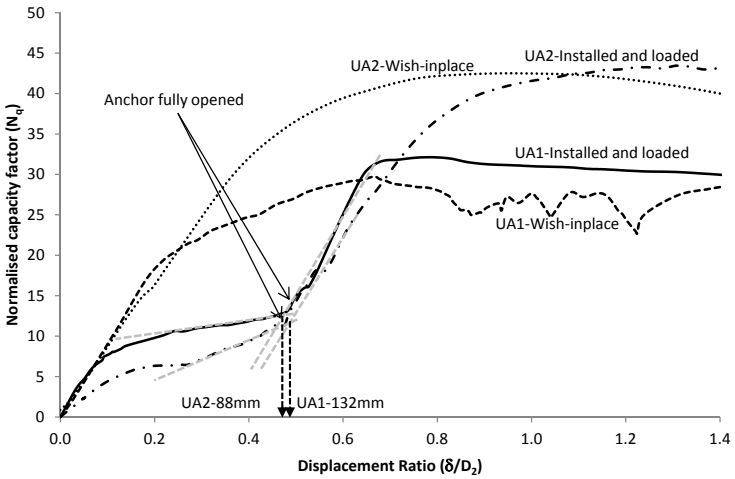

Figure 9. Wished-in-place and installed & loaded test comparison for both anchors with labels indicating point at which anchor had opened fully

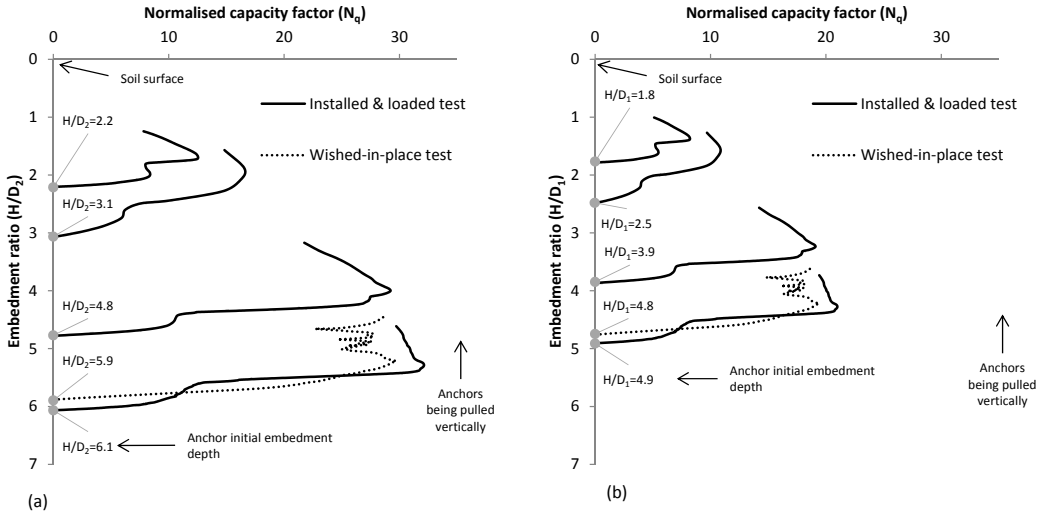

Figure 10. Normalised load-displacement plots for all UA1 (larger anchor) tests (a) normalised using equivalent diameter and actual anchor area and (b) normalised using width of fully opened anchor and projected area

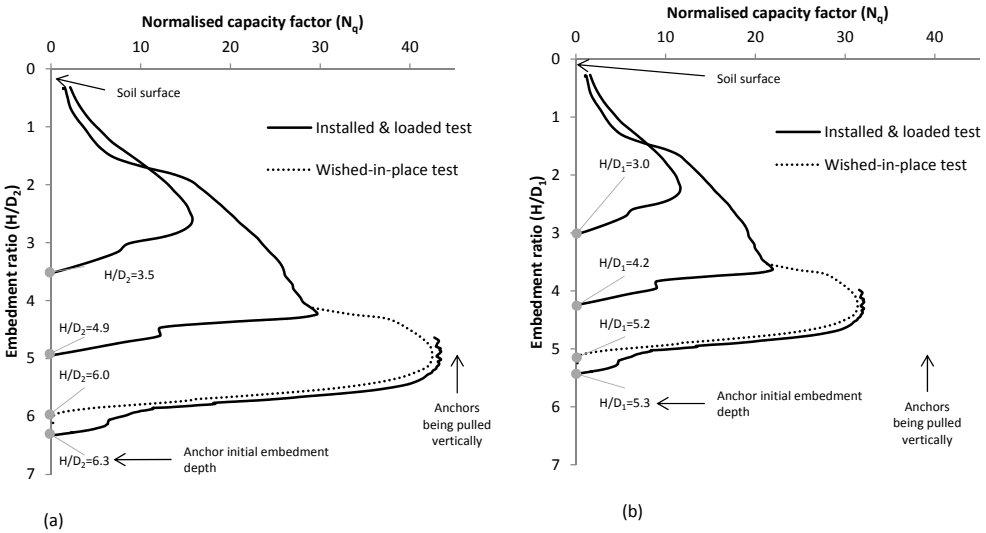

Figure 11. Normalised load-displacement plots for all UA2 (smaller anchor) tests (a) normalised using equivalent diameter and actual anchor area and (b) normalised using width of fully opened anchor and projected area

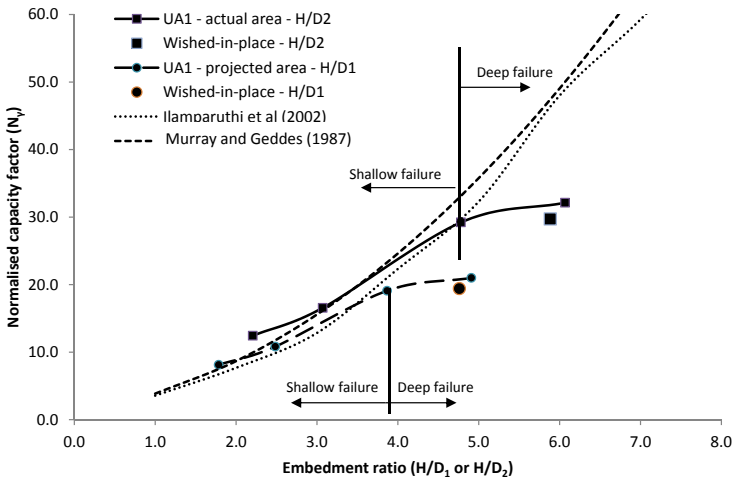

Figure 12. Normalised peak capacity for UA1 and analytical models

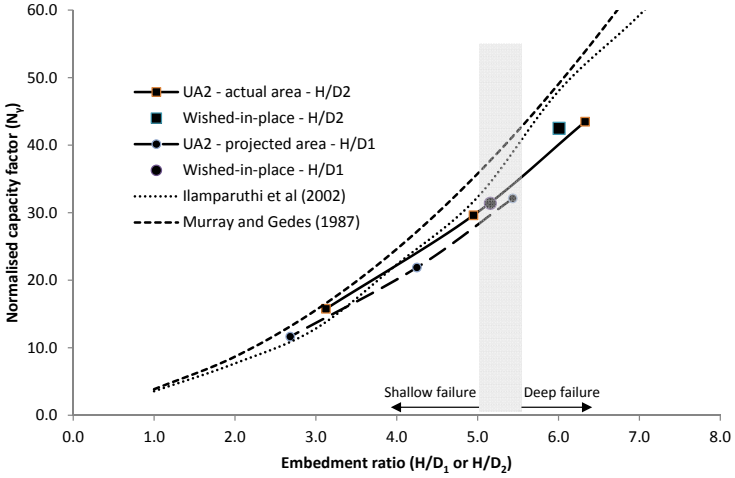

Figure 13. Normalised peak capacity for UA2 and analytical models

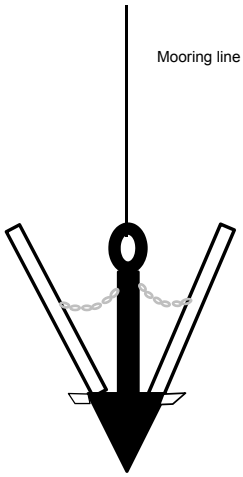

Figure 14. Possible alteration to anchor system